

Phase transition and dielectric properties of BaTiO₃ ceramics containing 10 mol% BaGeO₃

Roberto Köferstein*, Lothar Jäger, Mandy Zenkner, Stefan G. Ebbinghaus

Institut für Chemie/ Anorganische Chemie, Martin-Luther-Universität Halle-Wittenberg,

Kurt-Mothes Strasse 2, D-06120 Halle, Germany

* Corresponding author. Tel.: +49-345-5525630; Fax: +49-345-5527028.

E-mail address: roberto.koefenstein@chemie.uni-halle.de

Abstract. Dielectric properties and the cubic \rightleftharpoons tetragonal phase transition temperature of dense BaTiO₃ ceramics containing 10 mol% BaGeO₃, sintered between 840 and 1350 °C, have been investigated. The ceramic bodies were prepared from a nano-sized BaTi_{0.9}/Ge_{0.1}O₃ powder consisting of both BaTiO₃ and BaGeO₃ phases. The addition of BaGeO₃ leads to a reduction and broadening of the permittivity maximum, and to a small downshift of the paraelectric \rightleftharpoons ferroelectric phase transition temperature, compared to a pure BaTiO₃ ceramic. Lower sintering temperatures and thus small grain sizes of the ceramics cause an additional reduction of the maximum permittivity down to 2800. Both DTA and dilatometric measurements reveal also a downshifting of the phase transition temperature, as well as a decrease of the latent heat.

Keywords: ceramics; differential thermal analysis (DTA); dielectric properties; phase transitions

1. Introduction

Barium titanate (BaTiO_3) is one of the most frequently used ceramic materials in electronic devices due to its outstanding dielectric properties. Both, very fine-grained BaTiO_3 powders or sintering additives allow to reduce the sintering temperature. Sintering aids can influence not only the sintering temperature but also the dielectric/electrical properties of the final ceramics [1,2]. Yang [3] investigated the influence of CuO/BaO addition on the dielectric characteristic of BaTiO_3 ceramics. The effect of the sintering aid SiO_2 on the dielectric properties of BaTiO_3 or BaTiO_3 -based ceramics were examined by Freidenfels [4] and Lee [5], respectively. Freidenfels [4] reported that the addition of SiO_2 to BaTiO_3 decreases the dielectric permittivity. The dependency of the dielectric permittivity on glass-like additive of BaTiO_3 ceramics was investigated by Jeon [6].

The addition of germanates, like lead germanate, is used in industrial applications to produce heterophasic ceramic bodies [7,8]. Recently, we have investigated the influence of BaGeO_3 on the sintering behaviour and properties of fine- and coarse-grained BaTiO_3 powder compacts [9,10]. BaGeO_3 can be used as a sintering aid to reduce the sintering temperature of BaTiO_3 ceramics below 1000 °C. *Guha* and *Kolar* [11] studied the BaTiO_3 – BaGeO_3 system and they determined a eutectic composition of 68 mol% BaGeO_3 with a melting temperature of about 1120 ± 5 °C. The authors did not observe any shifting of the cubic \rightleftharpoons tetragonal phase transition temperature of BaTiO_3 (Curie temperature) by addition of BaGeO_3 , in agreement with the investigations by *Plessner* and *West* [12]. *Plessner* and *West* noticed only a reduction of the sharpness of the permittivity maximum. In contrast, *Pulvari* [13] and *Baxter* [14] found a small decrease in the Curie temperature with the addition of GeO_2 . Consequently, the knowledge about the effect of sintering additives on the dielectric properties of BaTiO_3 -based ceramics are important for potential technical applications.

The purpose of this study is to investigate the effects of the sintering additive BaGeO₃ on the dielectric characteristic of barium titanate ceramics. The influence of the sintering regimes and grain sizes has also been investigated. Additionally, the cubic \rightleftharpoons tetragonal phase transition has also been studied by dilatometric and DTA measurements.

2. Experimental

2.1. Material preparation

The preparation of a fine-grained BaTi_{0.9}/Ge_{0.1}O₃ powder and its characterization have been described elsewhere [9]. Briefly, a [Ba(HOC₂H₄OH)₄][Ti_{0.9}Ge_{0.1}(OC₂H₄O)₃] complex precursor was prepared by reaction of Ba(OH)₂·8H₂O, Ti(OⁱC₃H₇)₄ and Ge(OC₂H₅)₄ in 1,2-ethanediol. The resulting precursor was calcined by the following thermal treatment: heating to 550 °C with a heating rate of 10 K/min, slow heating with 1 K/min to 730 °C, dwelling time 30 min and followed by cooling at 10 K/min. After calcination the resulting nm-sized BaTi_{0.9}/Ge_{0.1}O₃ powder has a specific surface area of $S_{\text{BET}} = 16.9 \text{ m}^2/\text{g}$ ($d_{\text{av.}} = 61 \text{ nm}$) and mainly consists of a mixture of both BaTiO₃ and BaGeO₃ (denoted as: BaTi_{0.9}/Ge_{0.1}O₃). Chemical analyses (described in [9]) indicated a Ba/Ti ratio of 1.117 (calcd. 1.111) and a Ba/(Ti+Ge) ratio of 0.999 (calcd. 1.000). The preparation of the BaTiO₃ powder is similar to the preparation mentioned above [9,15]. The Ba/Ti ratio is 1.004 and the specific surface area is $S_{\text{BET}} = 15.0 \text{ m}^2/\text{g}$ ($d_{\text{av.}} = 66 \text{ nm}$). Detailed investigations of both the BaTi_{0.9}/Ge_{0.1}O₃ and BaTiO₃ powders are described elsewhere [9,10].

The powders were milled in propan-2-ol and pressed to disks (green density: 2.8–2.9 g/cm³) as described in [16] and sintered at various temperatures and sinter regimes.

2.2. Analytical methods

X-ray powder diffraction (XRD) patterns were recorded on a STOE STADI MP diffractometer at 25 °C using CoK α_1 radiation. Dilatometric investigations (thermal

expansion) were performed in a TMA 402 unit from *Netzsch*. The determination of the complex relative permittivity was achieved using an Impedance Analyzer 4192 Alf from *Hewlett Packard* in a temperature range between 14–140 °C and frequencies from 1–1000 kHz. As electrode material aluminium was deposited by evaporation. The samples were slowly heated to 140 °C, held for 3 h and then cooled down. Differential thermoanalytic (DTA) measurements were done using a STA 429 from *Netzsch* (Pt crucible, flowing air (30 ml/min)). Scanning electron microscope images were recorded with a *Philips* XL30 ESEM (Environmental Scanning Electron Microscope).

3. Results and discussion

In ref. [9,10] we have recently reported on the preparation and characterization of a nm-sized BaTiO₃ powder and resulting ceramic bodies containing 10 mol% BaGeO₃ (BaTi_{0.9}/Ge_{0.1}O₃). The ceramic bodies were obtained after conventional sintering (heating up to a certain temperature (rate 10 K/min), dwell for 1 h, and then cooling down with 10 K/min), as well as a 2-step sintering process (heating to a higher temperature (T₁, rate 10 K/min), then cooled (30 K/min) and held 50 h at a lower temperature (T₂)). SEM images of these ceramic bodies are shown in Fig. 1 (see also [9]). Grain sizes were determined on the basis of these images by lineal intercept technique [17]. BaTi_{0.9}/Ge_{0.1}O₃ ceramics show a heterogeneous grain size distribution. An overview of the ceramic bodies is given in Tab. 1. The relative densities of BaTi_{0.9}/Ge_{0.1}O₃ ceramic bodies (**1a–1e**) were related to the theoretical value of 5.85 g/cm³ [9] and of the BaTiO₃ ceramic body (**2**) to 6.02 g/cm³ [18]). As seen in Tab. 1 the addition of BaGeO₃ leads to a considerable reduction of the sintering temperature of BaTiO₃. As reported by *Guha* and *Kolar* [11], both BaGeO₃ and BaTiO₃ form solid solutions only up to a BaGeO₃ content of 1.8 mol% and they found a melting point of the eutectic at 1120 °C. The BaTi_{0.9}/Ge_{0.1}O₃ ceramic **1a** consists of tetragonal BaTiO₃, small amounts of orthorhombic

BaGeO₃ and Ba₂TiGe₂O₈. Moreover, the grains in sample **1a** are surrounded by a solidified eutectic melt, as a result of liquid phase sintering (see Fig. 1a) [9]. Whereas samples **1b–1e** consist of tetragonal BaTiO₃ and hexagonal BaGeO₃ (see ref. [10]) and they were obtained after solid state sintering. Results of dielectric measurements are shown in Fig. 2. The following data are related to the measurements of 1 kHz and collected from the cooling curve. Sample **2** (BaTiO₃) shows a sharp maximum of the relative permittivity (ϵ_r) at 128.4 ± 0.3 °C in agreement with earlier investigations [19,20,21,22,23]. The maximum of permittivity can be considered as a good indicator for the Curie temperature [21]. The addition of BaGeO₃ leads to a considerably smeared and lower permittivity maximum (Tab. 2). Ceramic **1a**, sintered at 1350 °C for 1 h, shows a significant shift of the curve maximum to 118.6 ± 0.3 °C. A reduction of the sintering temperature to 1100 °C (below the eutectic melt [11]) and thus a reduction of the grain size causes a small shift to lower temperatures of the curve maximum to 116.5 ± 0.3 °C (Tab. 2). A further lowering of the sintering temperature and grain size does not lead to a significant shift of the temperatures of the curve maxima. We observe that a decreasing grain size of the ceramics tends to a reduction of the height of the curve maximum. However, sample **1c** is an exception and we find a very small increase of the maximum permittivity (Tab. 2). A decreasing maximum permittivity with decreasing grain size is caused by a suppression of the spontaneous polarisation [24] and has been described by a theoretical model for PbTiO₃ by *Jiang* and *Bursill* [25]. Due to the broadening and reduction of the maximum permittivity, the maximum variation of the permittivity becomes lower with decreasing grain sizes. The maximum variation of permittivity in the whole temperature range (14–140 °C) for sample **1a** (grain size: 38 µm) is about 150 % of the room temperature permittivity, whereas sample **1e** (grain size: 1.2 µm) varies by about 70 %. For comparison, the coarse-grained BaTiO₃ ceramic (**2**) exhibits a large permittivity variation of 480 %. The permittivity at 70 °C of BaTi_{0.9}/Ge_{0.1}O₃ ceramics slightly increases with decreasing grain size (**1a–1c**). A further decrease of the grain size results in a decreasing permittivity (samples **1d**,

1e). A similar behaviour for pure BaTiO₃ ceramics was observed by *Shaikh* et al. [26] and *Arlt* et al. [38]. The temperature of the maximum permittivity of every ceramic body is almost unaffected by frequency within 0.4 K. The ceramic bodies (**1a-1e**) show slight differences in their dielectric losses ($\tan \delta$, not shown) because of their different sintering regimes and grain sizes. The dielectric loss for the fine grained ceramics (**1d**, **1e**) is less than 5% in the whole frequency range.

The cubic \rightleftharpoons tetragonal phase transition was also investigated by dilatometry and DTA measurements. The following data were obtained from the cooling curves (Tab. 2). Both methods show a small temperature difference of the transition temperatures between the heating and cooling phases (thermal hysteresis [27,28]). The phase transition temperatures determined from the cooling curves, are always shifted to lower temperatures compared to the heating curves.

The dilatometric measurements (thermal expansion) during the cooling phase (Fig. 3) show a sudden length change of the curve indicating the first-order phase transition from the cubic to the tetragonal modification. The cubic \rightleftharpoons tetragonal phase transition temperature was determined at the point of inflection of the measured curve. This procedure shows a phase transition at 120.5 ± 0.3 °C for BaTiO₃ (**2**). The BaTi_{0.9}/Ge_{0.1}O₃ ceramics reveal a small shift to lower transition temperatures (Tab. 2). Additionally, the reduction of the grain sizes and sintering temperatures causes also a slightly downward shifting of the transition temperature. The transition from an average grain size of 39 μm (**1a**) to 5.4 μm (**1b**) is connected with a small reduction of the phase transition temperature from 115.5 ± 0.3 °C to 111.5 ± 0.2 °C. A further grain reduction down to 1.2 μm (**1e**) is not affected by a significant change of the transition temperature.

DTA studies (Fig. 4) verify these results. The phase transition temperature was determined by the onset temperature of the DTA signal during the cooling phase [29]. We observe an onset temperature of 123.9 ± 0.3 °C for BaTiO₃, whereas sample **1a** causes an onset temperature of

116.6 ± 0.3 °C. At an average grain size from 5.4 to 1.2 μm (**1b–1e**) we obtain a constant transition temperature of about 115 °C. Since the transition temperatures of all samples are in a narrow range, the specific DTA peak area is in good approximation proportional to the latent heat (ΔH) during the phase transition [30]. The latent heat of sample **1a** and **1b** does not differ from each other and is about 72 % of the value of BaTiO_3 (**2**). Additionally, the latent heat decreases continuously with decreasing grain sizes (sintering temperatures) of the $\text{BaTi}_{0.9}/\text{Ge}_{0.1}\text{O}_3$ ceramics. From sample **1a** to sample **1e** the latent heat is reduced by 27 %. That means, the small grain sizes of ceramics **1c–1e** lead to a lower latent heat during the cubic \rightleftharpoons tetragonal phase transition. It is known that small grain sizes cause a reduction of the tetragonality of the BaTiO_3 unit cell [21,31,35]. A decreasing c/a ratio (c and a being lattice parameters) by small grain sizes of $\text{BaTi}_{0.9}/\text{Ge}_{0.1}\text{O}_3$ ceramics can be seen in a lower splitting of the (112/211) reflection of the BaTiO_3 phase (Fig. 5). In the same way, we observe a decrease of the length change during the dilatometric measurements of the cubic \rightleftharpoons tetragonal phase transitions. These effects are mainly grain size effects and have also been observed in pure BaTiO_3 ceramics [20,21,32,33,34,35,36,37,38] and can be explained by intrinsic size effects (internal stress [39]). However, the variation of permittivity and transition temperature with grain sizes is a complex phenomenon. *Perriat* et al. [40] interpreted the variation of permittivity and Curie temperature with grain sizes by a thermodynamic model considering the surface free energy. Whereas, *Lee* et al. [27] pointed out that sintering temperatures influence the Curie temperature because of Schottky defects and *Kuwabara* et al. [22] reported also that oxygen vacancies are responsible for changing the Curie temperature.

As mentioned above, the transition from a coarse-grained BaTiO_3 ceramic body (**2**) to coarse-grained $\text{BaTi}_{0.9}/\text{Ge}_{0.1}\text{O}_3$ ceramics (**1a**, **1b**) is also associated with a decreasing latent heat, a slightly smaller length change, and a reducing and broadening permittivity maximum. We suppose that the small incorporation of Ge^{4+} into the BaTiO_3 structure (Ge^{4+} occupying the Ti^{4+} sites [11]) causes these effects mainly. *Hennings* and *Schnell* [41] found also a decreasing

latent heat by gradually incorporation of Zr^{4+} into BaTiO_3 . A shift of the cubic \rightleftharpoons tetragonal phase transition to lower temperatures as well as a reduction of the maximum permittivity by addition of BaGeO_3 were also observed in $\text{BaTi}_{1-x}\text{Sn}_x\text{O}_3$ ceramics [42].

4. Conclusion

BaGeO_3 acts as a sintering aid for BaTiO_3 ceramics to reduce the sintering temperature. It can be seen that BaGeO_3 leads not only to a reduction of the sintering temperature, but the sintering aid also strongly influences the dielectric properties of the BaTiO_3 ceramics. In particular the addition of BaGeO_3 leads to a strong reduction of the permittivity maximum and of the sharpness of the curve maximum, i.e. the paraelectric \rightleftharpoons ferroelectric phase transition becomes diffuser. Whereas, pure BaTiO_3 shows a very sharp maximum of the permittivity during the phase transition. Additionally, we observe only a small shift of the maximum permittivity to lower temperatures, compared with pure BaTiO_3 ceramics. Moreover, the dielectric properties are also influenced by grain sizes. A decreasing grain size of $\text{BaTi}_{0.9}/\text{Ge}_{0.1}\text{O}_3$ ceramics also reduces the permittivity maximum and thus the paraelectric \rightleftharpoons ferroelectric phase transition is smeared. The influence of BaGeO_3 as well as grain sizes is also reflected in DTA and dilatometric investigations. It can be observed that $\text{BaTi}_{0.9}/\text{Ge}_{0.1}\text{O}_3$ ceramics show a lower latent heat and a lower length change (thermal expansion) during the cubic \rightleftharpoons tetragonal phase transition than pure BaTiO_3 ceramics. With decreasing grain sizes the crystal structure of $\text{BaTi}_{0.9}/\text{Ge}_{0.1}\text{O}_3$ becomes slightly less tetragonal, therefore the latent heat of the phase transition is gradually reduced, mainly caused by intrinsic size effects.

Acknowledgements

The authors thank Dr. Th. Müller for dilatometric and DTA measurements, as well as for his helpful discussions. Financial support by the Federal State Saxony-Anhalt (Cluster of Excellence "Nanostructured Materials") is gratefully acknowledged.

Table 1

Overview of the ceramic bodies used.

Composition	Sample	Sintering regime	Relative density (%)	Grain size (μm)	
				average [13]	range
Conventional sintering procedure					
BaTiO ₃	2	1350 °C, 1 h	93	14	7–37
BaTi _{0.9} /Ge _{0.1} O ₃	1a	1350 °C, 1 h	94	39	11–60
BaTi _{0.9} /Ge _{0.1} O ₃	1b	1100 °C, 1 h	95	5.4	1.5–13
BaTi _{0.9} /Ge _{0.1} O ₃	1c	1050 °C, 1 h	96	3.3	0.9–5
2-step sintering procedure					
BaTi _{0.9} /Ge _{0.1} O ₃	1d	T ₁ = 950 °C, T ₂ = 850 °C, 50 h	92	1.4	0.6–3
BaTi _{0.9} /Ge _{0.1} O ₃	1e	T ₁ = 970 °C, T ₂ = 840 °C, 50 h	90	1.2	0.6–2

Table 2

Maximum permittivity and related temperature measured at 1 kHz. Cubic \rightleftharpoons tetragonal phase transition temperature (T_{CT}) determined by dilatometry and DTA.

Sample	Maximum permittivity	Temperature for maximum permittivity [°C]	T _{CT} (dilatometry) [°C] ¹	T _{CT} (DTA) [°C] ²
2	10000	128.4 ± 0.3	120.5 ± 0.3	123.9 ± 0.2
1a	4600	118.6 ± 0.3	115.5 ± 0.3	116.6 ± 0.3
1b	4300	116.5 ± 0.3	111.5 ± 0.2	114.7 ± 0.2
1c	4900	116.3 ± 0.3	111.3 ± 0.3	114.8 ± 0.2
1d	3400	116.5 ± 0.3	111.9 ± 0.4	115.2 ± 0.2
1e	2800	115.8 ± 0.3	111.4 ± 0.3	114.8 ± 0.2

The data were determined from the cooling curves.

1) temperature at the point of inflection, 2) onset temperature

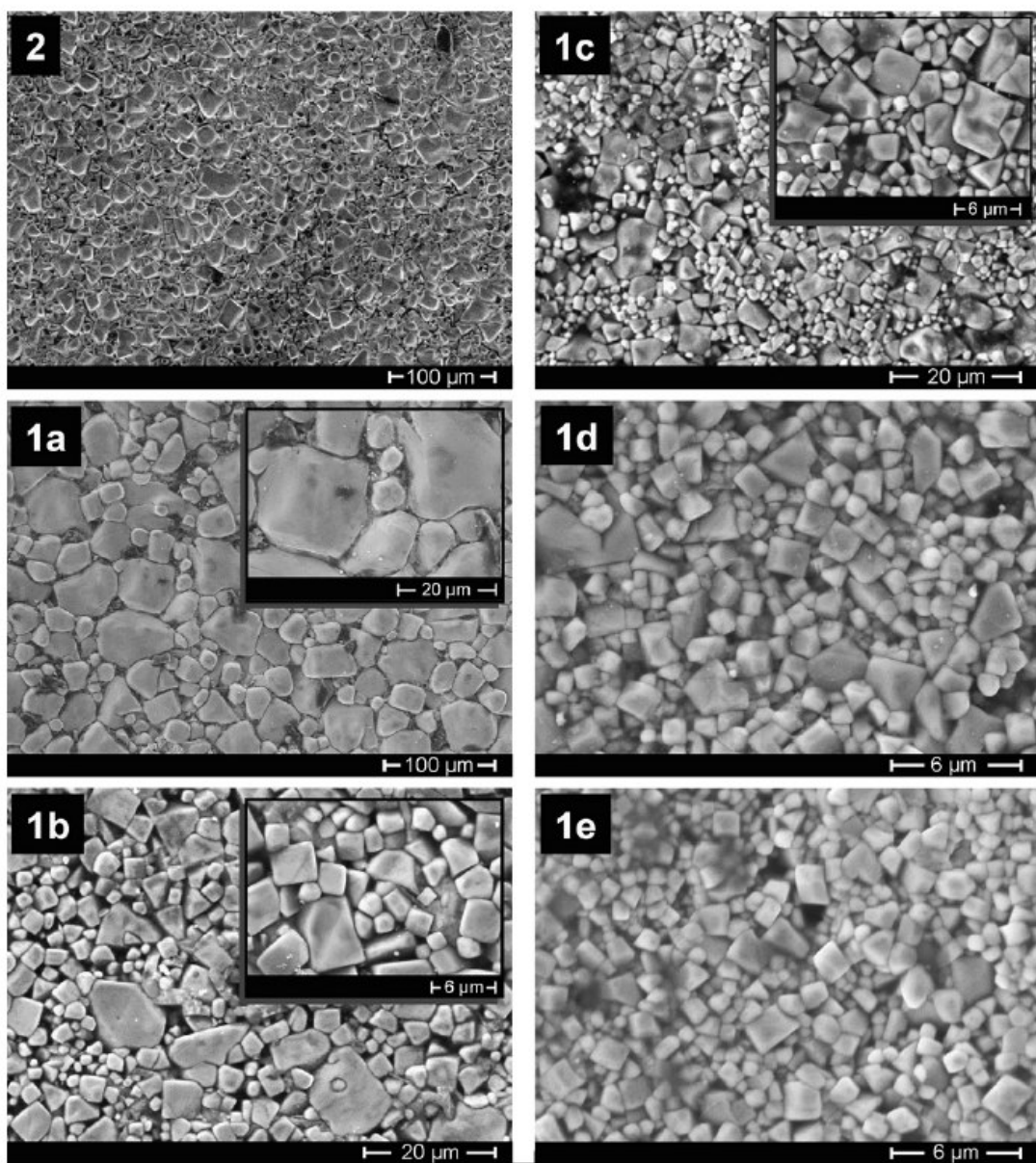


Fig. 1. SEM images of the surface of BaTiO_3 (2) and $\text{BaTi}_{0.9}/\text{Ge}_{0.1}\text{O}_3$ (1a–1e) ceramic bodies.

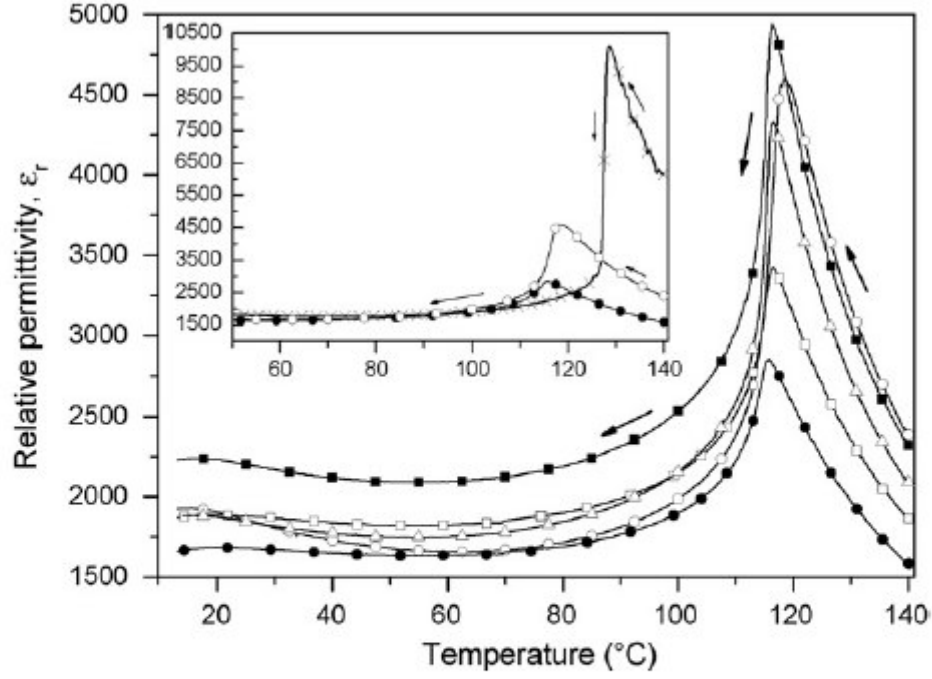


Fig. 2. Real part of the relative permittivity (ϵ_r) at a frequency of 1 kHz versus temperature of $\text{BaTi}_{0.9}/\text{Ge}_{0.1}\text{O}_3$ ceramics (**1a–1e**) and BaTiO_3 (**2**). (○) **1a**; (△) **1b**; (■) **1c**; (□) **1d**; (●) **1e**; (×) **2**. The figure shows the cooling curves (average cooling rate 0.18 K min^{-1}).

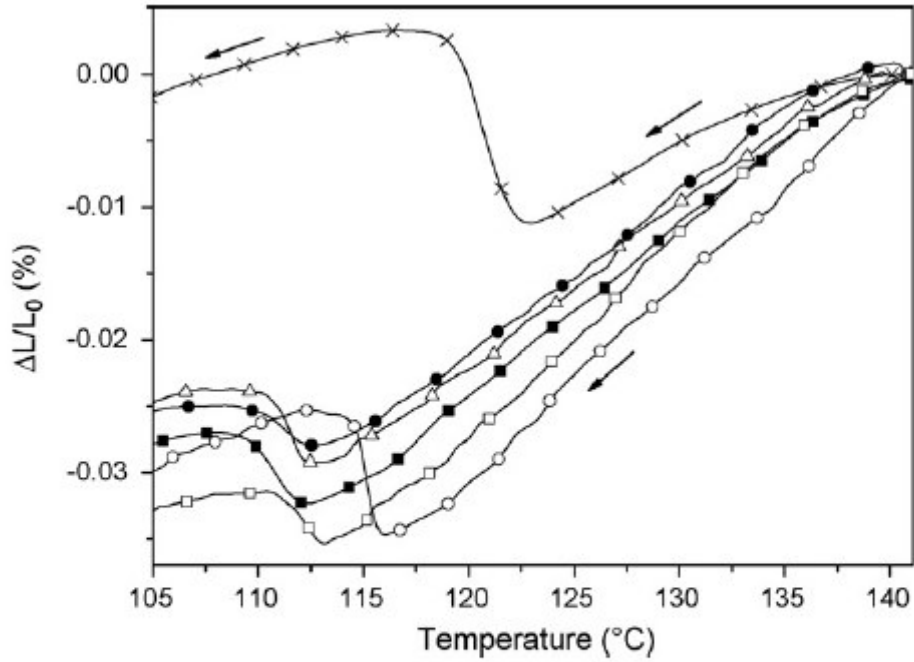


Fig. 3. Dilatometric measurements of the expansion of $\text{BaTi}_{0.9}/\text{Ge}_{0.1}\text{O}_3$ ceramics (**1a–1e**) and BaTiO_3 (**2**) during the cubic \rightleftharpoons tetragonal phase transition. (○) **1a**; (△) **1b**; (■) **1c**; (□) **1d**; (●) **1e**; (×) **2**. The figure shows the cooling curves (cooling rate 2.0 K min^{-1}).

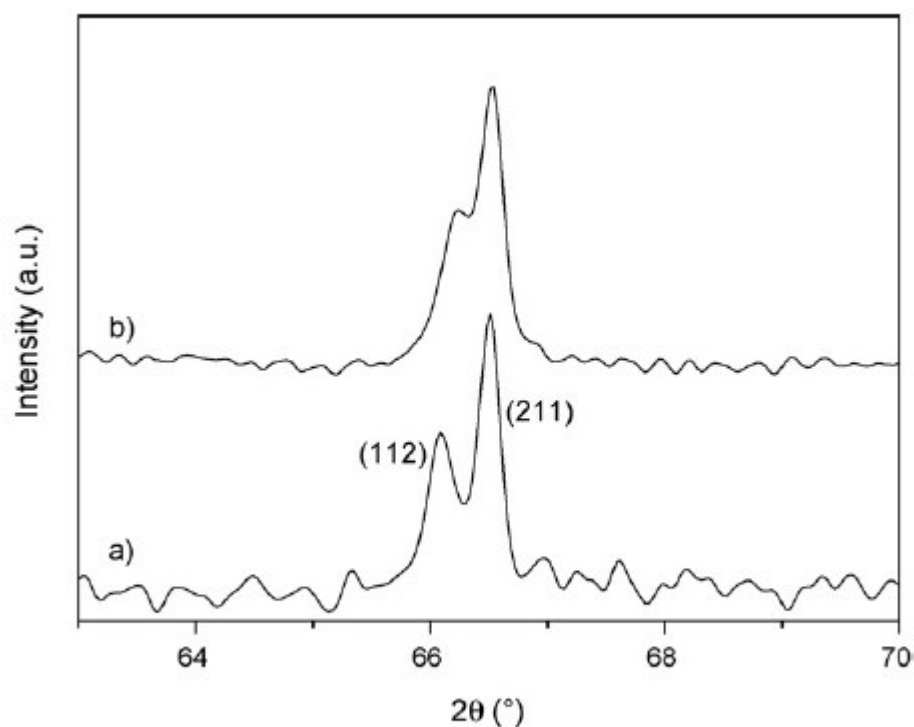


Fig. 5. X-ray powder diffraction patterns (recorded at 25 °C) of (112) and (211) reflections for BaTi_{0.9}/Ge_{0.1}O₃ ceramics **1a** (a) and **1e** (b).

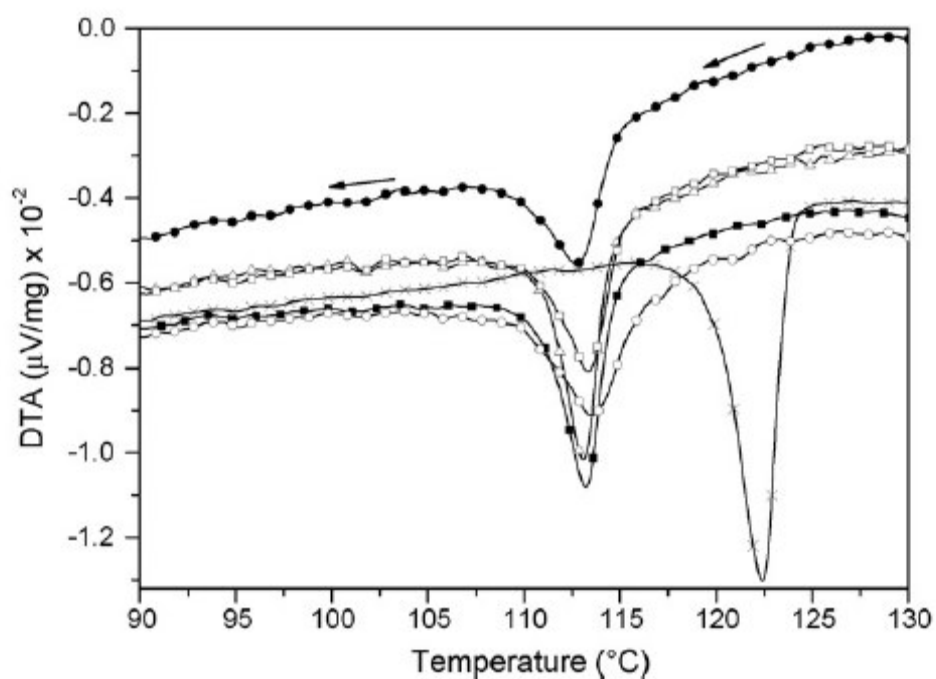


Fig. 4. DTA traces of BaTi_{0.9}/Ge_{0.1}O₃ ceramics (**1a–1e**) and BaTiO₃ (**2**) during the cubic \rightleftharpoons tetragonal phase transition. (○) **1a**; (Δ) **1b**; (■) **1c**; (□) **1d**; (●) **1e**; (×) **2**. The figure shows the cooling curves (cooling rate 2.0 K min⁻¹).

References

- [1] H.-P. Jeon, S.-K. Lee, S.-W. Kim, D.-K. Choi, *Mater. Chem. Phys.* 94 (2005) 185–189.
- [2] G. Liu, R. D. Roseman, *J. Mater. Sci.* 34 (1999) 4439–4445.
- [3] C.-F. Yang, *Ceram. Inter.* 24 (1998) 341–346
- [4] E. Z. Freidenfelds, V. Y. Fricberg, Y. Y. Kruchan, *Uch. Zap. Rzhsk. Politekh. Inst.* 2 (1959) 115–127
- [5] Y. C Lee, W. Lu, S. H Wang, C. H. W Lin, *Inter. J. Miner. Metall. Mater.* 16 (2009) 124–127
- [6] H.-P. Jeon, S.-K. Lee, S.-W. Kim, D.-K. Choi, *Mater. Chem. Phys.* 94 (2005) 185–189
- [7] D. A. Payne, S. M. Park, *Heterophasic ceramic composition*. U.S. Patent No. 4,218,723, (1980).
- [8] M. S.-H. Chu, J. Bultitude, C. Hood, K. L. Nimmo, M. Rand, *Temperature stable dielectric*. EU Patent No. EP 0,731,066,A1 (1996).
- [9] R. Köferstein, L. Jäger, M. Zenkner, H.-P. Abicht, *J. Mater. Sci.* 43 (2008) 832–838.
- [10] R. Köferstein, L. Jäger, M. Zenkner, T. Müller, H.-P. Abicht, *Mater. Chem. Phys.* 112 (2008) 531–535.
- [11] J. P. Guha, D. Kolar, *J. Mater. Sci.* 7 (1972) 1192–1196.
- [12] K. W. Plessner, R. West, *Proc. Phys. Soc.* B68 (1955) 1150–1151.
- [13] C. F. Pulvari, *J. Am. Ceram. Soc.* 42(8) (1959) 355–363.
- [14] P. Baxter, N. J. Hellicar, B. Lewis, *J. Am. Ceram. Soc.* 42 (1959) 465–471.
- [15] R. Köferstein, L. Jäger, V. Lorenz, H.-P. Abicht, J. Woltersdorf, E. Pippel, H. Görls, *Solid State Sci.* 7 (2005) 1280–1288.

-
- [16] R. Köferstein, L. Jäger, M. Zenkner, H.-P. Abicht, *Thermochim. Acta* 457 (2007) 55–63.
- [17] J. C. Wurst, J. A. Nelson, *J. Am. Ceram. Soc.* 55 (1972) 109.
- [18] H. T. Evans jr, *Acta Cryst.* 14 (1961) 1019–1026.
- [19] K. Kinoshita, A. Yamaji, *J. Appl. Phys.* 47 (1976) 371–373.
- [20] T.-T. Fang, H.-L. Hsieh, F.-S. Shiau, *J. Am. Ceram. Soc.* 76 (1993) 1205–1211.
- [21] Z. Zhao, V. Buscaglia, M. Viviani, M. T. Buscaglia, L. Mitoseriu, A. Testino, M. Nygren, M. Johnsson, P. Nanni, *Phys. Rev. B* 70 (2004) 024107-1pp.
- [22] M. Kuwabara, H. Matsuda, N. Kurata, E. Matsuyama, *J. Am. Ceram. Soc.* 80 (1997) 2590–2596.
- [23] G. W. Marks, L.A. Monson, *Ind. Eng. Chem.* 47 (1955) 1611–1620.
- [24] H. T. Martirena, J. C. Burfoot, *J. Phys. C: Solid State Phys.* 7 (1974) 3182–3191.
- [25] B. Jiang, L. A. Bursill, *Phys. Rev. B*, 60 (1999) 9978–9982.
- [26] A. S. Shaikh, R. W. Vest, G. M. Vest, *IEEE Trans. Ultrason. Ferroelec. Freq. Controll*, 36 (1989) 407–412.
- [27] S. Lee, Z.-K. Liu, M.-H. Kim, C. A. Rendall, *J. Appl. Phys.* 101 (2007) 054119-1 pp.
- [28] Y. He, *Thermochim. Acta*, 419 (2004) 135–141.
- [29] G. W. H. Höhne, H. K. Cammenga, W. Eysel, E. Gmelin, W. Hemminger, *Thermochim. Acta*, 160 (1990) 1–12.
- [30] T. Ozawa, *Bull. Chem. Soc. Jpn.* 39 (1966) 2071–2085.
- [31] S.-W. Kwon, D.-H. Yoon, *J. Eur. Ceram. Soc.* 27 (2007) 247–252
- [32] T. Takeuchi, M. Tabuchi, K. Ado, K. Honjo, O. Nakamura, H. Kageyama, Y. Suyama, N. Ohtori, M. Nagasawa, *J. Mater. Sci.* 32 (1997) 4053–4060.
- [33] M. H. Frey, D. A. Payne, *Phys. Rev. B* 54 (1996) 3158–3168.

-
- [34] B. G. Begg, E. R. Vance, J. Nowotny, *J. Am. Ceram. Soc.* 77 (1994) 3186–3192.
- [35] V. Buscaglia, M. T. Buscaglia, M. Viviani, L. Mitoseriu, P. Nanni, V. Trefiletti, P. Piaggio, I. Gregora, T. Ostapchuk, J. Pokorný, J. Petzelt, *J. Eur. Ceram. Soc.* 26 (2006) 2889–2898.
- [36] Y. Sakabe, N. Wada, Y. Hamaji, *J. Korean Phys. Soc.* 32 (1998) S260–S264.
- [37] T. Takeuchi, K. Ado, T. Asai, H. Kageyama, Y. Saito, C. Masquelier, O. Nakamura, *J. Am. Ceram. Soc.* 77 (1994) 1665–1668.
- [38] D. Arlt, D. Hennings, G. de With, *J. Appl. Phys.* 58 (1985) 1619–1625.
- [39] W. R. Buessem, L. E. Cross, A. K. Goswami, *J. Am. Ceram. Soc.* 49 (1966) 33–36.
- [40] P. Perriat, J. C. Niepce, G. Caboche, *J. Thermal Anal.* 43 (1994) 635–649.
- [41] D. Hennings, A. Schnell, *J. Am. Ceram. Soc.* 65 (1982) 539–544.
- [42] M. Zenkner, L. Jäger, R. Köferstein, H.-P. Abicht, *Solid State Sci.* 10 (2008) 1556–1562.